Published in final edited form as:
Nature. 2020 August ; 584(7821): E20–E28. doi:10.1038/s41586-020-2522-3.

APP gene copy number changes reflect exogenous contamination

Junho Kim[1], **Boxun Zhao**[1], **August Yue Huang**[1], **Michael B. Miller**[1,2,3], **Michael A. Lodato**[1,2,4], **Christopher A. Walsh**[1,2,*], **Eunjung Alice Lee**[1,*]

[1]Division of Genetics and Genomics, Manton Center for Orphan Disease, Boston Children's Hospital, Boston, MA, USA; Department of Pediatrics, Harvard Medical School, Boston, MA, USA; and Broad Institute of MIT and Harvard, Cambridge, MA, USA.

[2]Howard Hughes Medical Institute, Boston Children's Hospital, Boston, MA, USA and Department of Neurology, Harvard Medical School, Boston, MA, USA

[3]Department of Pathology, Brigham and Women's Hospital, Harvard Medical School, Boston, MA, USA.

[4]Current Address: Department of Cell, Molecular, and Cancer Biology, University of Massachusetts Medical School, Worcester, MA, USA

Various types of somatic mutations occur in cells of the human body and cause human diseases including cancer and some neurological disorders[1]. Recently, Lee et al.[2] (hereafter "the Lee study") reported somatic copy number gains of the *APP* gene, a known risk locus of Alzheimer's disease (AD), in 69% and 25% of neurons of AD patients and controls. The authors argue that the mechanism of these copy number gains was somatic integration of *APP* mRNA into the genome, creating what they called genomic cDNA (gencDNA). Our reanalysis of the data from the Lee study and two additional whole exome sequencing (WES) datasets by the authors of the Lee study[3] and Park et al.[4] revealed evidence that *APP* gencDNA originates mainly from exogenous contamination by *APP* recombinant vectors, nested PCR products, and human and mouse mRNA, respectively, rather than from true somatic integration of endogenous *APP*. We further present our own single-cell whole genome sequencing (scWGS) data that show no evidence for somatic *APP* retrotransposition in AD neurons or in neurons from normal individuals of various ages.

We examined the original *APP*-targeted sequencing data from the Lee study to investigate sequence features of *APP* retrotransposition. These expected features included (a) reads

[*]to whom correspondence should be addressed. Christopher.Walsh@childrens.harvard.edu or EAlice.Lee@childrens.harvard.edu.

Author contributions

J.K. and E.A.L. conceived and designed the study. J.K. and B.Z. designed the *APP* vector PCR and sequencing, and B.Z. performed the PCR and sequencing. M.B.M. and M.A.L. performed single-neuron sorting and sequencing. J.K. and A.Y.H. performed bioinformatic analyses. E.A.L and C.A.W supervised the study. J.K., B.Z., M.B.M., M.A.L., C.A.W., and E.A.L. wrote the manuscript.

Competing interests

Declared none.

Code availability

Implemented custom code for the estimation of clipped read fractions and the detection of intra-exon junctions (IEJs) is available at https://sourceforge.net/projects/somatic-app-analysis/.

spanning two adjacent *APP* exons without intervening intron sequence, which would indicate processed *APP* mRNA, and (b) clipped reads, which are reads spanning the source *APP* and new genomic insertion sites, thus manifesting partial alignment to both the source and target site (Extended Data Fig. 1a). The first feature is the hallmark of retrogene or pseudogene insertions, and the second is the hallmark of RNA-mediated insertions of all kinds of retroelements, including retrogenes as well as LINE1 elements. We indeed observed multiple reads spanning two adjacent *APP* exons without the intron; however, we could not find any reads spanning the source *APP* and a target insertion site. Surprisingly, we found multiple clipped reads at both ends of the *APP* coding sequence (CDS) containing the multiple cloning site of the pGEM-T Easy Vector (Promega), which indicates external contamination of the sequencing library by a recombinant vector carrying an insert of *APP* coding sequence (Fig. 1a). The *APP* vector we found here was not used in the Lee study, but rather had been used in the same laboratory when first reporting genomic *APP* mosaicism[5], suggesting carryover from the prior study.

Recombinant vectors with inserts of gene coding sequences (typically without introns or untranslated regions (UTRs)) are widely used for functional gene studies. Recombinant vector contamination in next-generation sequencing is a known source of artifacts in somatic variant calling, as sequence reads from the vector insert confound those from the endogenous gene in the sample DNA[6]. We have identified multiple incidences of vector contamination in next-generation sequencing datasets from different groups, including our own laboratory (Extended Data Fig. 1b), demonstrating the risk of exposure to vector contamination. In an unrelated study on somatic copy number variation in the mouse brain[7], from the same laboratory that authored the Lee study, we found contamination by the same human *APP* pGEM-T Easy Vector in mouse single-neuron WGS data (Extended Data Fig. 1c). We also observed another vector backbone sequence (pTripIEx2, SMART cDNA Library Construction Kit, Clontech) with an *APP* insert (Extended Data Fig. 1c, magnified panel) in the same mouse genome dataset, indicating repeated contamination by multiple types of recombinant vectors in the laboratory.

PCR-based experiments with primers targeting the *APP* coding sequence (e.g., Sanger sequencing and SMRT sequencing) are unable to distinguish *APP* retrocopies from vector inserts (Fig. 1a, upper panel). Therefore, to definitively distinguish the three potential sources of *APP* sequencing reads (original source *APP*, retrogene copy, and vector insert), it is necessary to study non-PCR-based sequencing data (*e.g.*, SureSelect hybrid-capture sequencing) and examine reads at both ends of the *APP* coding sequence. Such data can help to assess whether the clipped sequences map to a new insertion site or to vector backbone sequence (Fig. 1a, lower panel). From the SureSelect hybrid-capture sequencing data in the Lee study, we directly measured the level of vector contamination by calculating the fraction of the total read depth at both ends of the *APP* coding sequence comprised by clipped reads containing vector backbone sequences (Fig. 1b, red dots). Similarly, we measured the clipped read fraction at each *APP* exon junction, which indicates the total amount of *APP* gencDNAs (either from *APP* retrocopies or vector inserts) (Fig. 1b, black dots). The average clipped read fraction at coding sequence ends that contained vector backbones (1.2%, red dots) was comparable to the average clipped read fraction at exon junctions (1.3%, black dots; P=0.64, Mann-Whitney U test), suggesting vector contamination as the primary source of the clipped reads across all the exon junctions. Even including these vector-originating reads, all the fractions at every junction are far below the conservative estimate of 16.5% gencDNA contribution based on the Lee study's DISH experimental results, which are from the same samples (see Supplementary Information for more details on the discrepancy between sequencing and DISH results). It is incumbent on the authors to provide explanation for this significant inconsistency. Moreover, if the clipped reads were from endogenous retrocopies, the clipped and non-clipped reads would be expected to be of similar insert (DNA fragment) size distribution; however, we observed that in the Lee study, the clipped reads were of significantly smaller and far more homogeneous insert size distribution than the non-clipped reads that were from original source *APP*, thus demonstrating the foreign nature of the clipped reads ($P < 2.2 \times 10^{-16}$, Mann-Whitney U test; Extended Data Fig. 2a–c, see Supplementary Information). Finally, we found no direct evidence supporting the existence of true *APP* retrogene insertions, such as clipped and discordant reads near the *APP* UTR ends that mapped to a new insertion site, or clipped reads with polyA tails at the 3' end of the UTR although the sequencing depth of UTRs was over 500x. Given that the hybrid capture experiment appears properly designed to detect *APP* gencDNA, the absence of any *bona fide* insertion signal suggests the absence of true *APP* gencDNA and that a majority of *APP*-gencDNA-supporting reads originated from *APP* vector contamination.

The authors of the Lee study have subsequently generated WES datasets from the brain samples of six AD patients and one non-AD control (SRA Accession: PRJNA558504), and reported multiple reads spanning *APP* exons without introns as evidence of somatic *APP* gencDNA[3]. We confirmed this in the data, but again, found not a single read spanning the source *APP* and any insertion sites. Instead, the data revealed anomalous patterns in a subset of reads supporting *APP* gencDNA. Those reads spanning exons 1 and 18 were aligned to the exact same start and end positions with the same read pair orientation (Fig. 2a), which is unlikely to occur in non-PCR-based exome capture sequencing. We found that the two aligned positions within exons 1 and 18 exactly match the target sites of the nested PCR primers used in the original Lee study (1–18N, Supplementary Table 1 in the Lee study). The only explanation for this observation is the contamination of the WES library by nested PCR products from the original APP study. This finding raises serious concerns that *APP* PCR products may also have contaminated the genomic DNA samples and were fragmented and sequenced together, generating more gencDNA-compatible reads for which we are unable to clarify the source. We also identified two unannotated (*i.e.,* absent in the gnomAD) single-nucleotide variants in all *APP*-cDNA-supporting reads in the two independent WES libraries pooled from six AD patient samples, which is very unlikely to be observed in different individuals, thus supporting the possibility that the *APP* cDNA originated from the same external source (Fig. 2b).

An independent study by Park et al.[4] has recently presented a small fraction of reads supporting *APP* cDNA in deep WES datasets from AD brain samples (SRA Accession: PRJNA532465; Supplementary Fig. 12 in the study). This data was free from vector contamination, but we found evidence of genome-wide human mRNA contamination, predominantly in the WES datasets with reported *APP* cDNA supporting reads. We note that their analysis of somatic single-nucleotide variants (SNVs) is likely to be unaffected by this contamination due to their visual inspection and stringent filtering of known germline SNVs.

For each AD brain sample, we counted the number of genes with potential somatic retrotransposition events by checking whether a gene had cDNA-supporting reads (*i.e.*, reads connecting two adjacent exons, skipping the intervening intron) at more than two different exon junctions in the brain sample but not in the matched blood sample from the same patient (see Supplementary Methods). All WES datasets reported by the authors to have *APP* cDNA showed an extremely high number of other genes in addition to *APP* with cDNA-supporting reads (40–2,995 genes) (Fig. 2c). Considering that far less than one somatic retrogene insertion per sample would be expected for human cells, even for human cancers with a high rate of somatic LINE1 retrotransposition (*e.g.*, lung and colorectal cancer)[8], this result strongly suggests that cDNA-supporting reads could not have originated from true somatic insertions of hundreds to thousands of retrogenes but rather supports the presence of genome-wide human mRNA contamination. We also found cDNA-supporting reads, including a subset of *APP* cDNA-supporting reads, originating from mouse mRNA, additionally confirming mRNA contamination of the data (Fig. 2d and Supplementary Fig. 1). We observed mRNA contamination in one cell in our scWGS data (see Supplementary Information). Neither Park et al. (per personal communication) nor we had performed any mRNA experiments, suggesting the possibility of contamination from some source outside the research laboratories, such as the sequencing facility. Taken together, we found no evidence of genuine *APP* genomic cDNA either in the new WES data from the Lee study authors, or in the independent Park et al. data. These findings highlight pervasive exogenous contamination in next-generation sequencing experiments, even with high quality control standards, and emphasizes the need for rigorous data analysis to mitigate these significant sources of artifacts.

The Lee study reported numerous novel forms of *APP* splice variants with intra-exon junctions (IEJs) with greater diversity in AD patients than controls. The authors also presented short sequence homology (2–20 bp) at IEJs suggesting a microhomology-mediated end-joining as a mechanism underlying IEJ formation. It is well known that microhomology can predispose to PCR artifacts[9], and the Lee study performed a high number of PCR cycles in their experimental protocol (40 cycles). Thus, we tested the hypothesis that the IEJs in the Lee study could have arisen as PCR artifacts from the PCR amplification of a contaminant. To do so, we repeated in our laboratory both RT-PCR and PCR assays following the Lee study protocol using recombinant vectors with two different *APP* isoforms (*APP*-751, *APP*-695), and using the reported PCR primer sets with three different PCR enzymes as described in their study (see Supplementary Information). Indeed, with all combinations of *APP* inserts and PCR enzymes, we observed chimeric amplification bands with various sizes, clearly distinct from the original *APP* inserts (Fig. 1c, Extended Data Fig. 3a). We further sequenced these non-specific amplicons and confirmed that they contained numerous IEJs of *APP* inserts (Supplementary Table 1). 12 of 17 previously reported IEJs in the Lee study were also found from our sequencing of PCR artifacts (Fig. 1c and Extended Data Fig. 3b). Our observations suggest that the novel *APP* variants with IEJs from the Lee study might have originated from contaminants as PCR artifacts. This possibility is corroborated by the fact that IEJ-supporting reads were completely absent in the hybrid-capture sequencing data from the Lee study, and that reads supporting an IEJ in the new WES dataset by the authors originated from external nested *APP* PCR products (Fig. 2a).

To independently investigate potential *APP* gencDNA, we searched for somatic *APP* retrogene insertions in our independent scWGS data from AD patients and normal controls. Briefly, single-neuronal nuclei were isolated using NeuN staining followed by FACS sorting, whole-genome amplified using multiple displacement amplification (MDA), and finally whole-genome sequenced at 45X mean depth[10]. The dataset consists of a total of 64 scWGS datasets from 7 AD patients with Braak stage V and VI disease, along with 119 scWGS datasets from 15 unaffected control individuals, some of which have been previously published[11]. Our previous studies and those by other groups[10,12–14] have successfully detected and fully validated *bona fide* somatic insertions of LINE1 by capturing distinct sequence features in scWGS data, demonstrating the high resolution and accuracy of scWGS-based retrotransposition detection. Therefore, if a retrogene insertion had occurred, we should have been able to observe distinct sequence features at the source retrogene site: increased exonic read-depth, read clipping at exon junctions, poly-A tail at the end of the 3' UTR, and discordant read pairs spanning exons (Extended Data Fig. 1a). We indeed clearly captured these features at the existing germline retrogene insertions, such as the *SKA3* pseudogene insertion (Fig. 3a). If present, somatic events should be able to be detected as heterozygous germline variants in scWGS; however, our analysis revealed no evidence of somatic *APP* retrogene insertions in any cell. In contrast, we observed that in both patients (AD3 and AD4) carrying germline insertions of *SKA3* and the patient (AD2) carrying a germline insertion of *ZNF100*, there was a clear increase in exonic read depth relative to introns, as would signal for polymorphic germline retrogene insertions (Fig. 3b). We observed no such read depth increase for *APP* in our 64 AD and 119 normal single-neuron WGS profiles, confirming that we found no evidence of *APP* retrogene insertions in human neurons.

In summary, our analysis of the original sequencing data from the Lee study, the new WES data from the same authors, and the WES data from the independent Park study, as well as of our own scWGS data suggests that somatic *APP* retrotransposition does not frequently occur either in AD or control neurons. Rather, the reported evidence of *APP* retrocopies appears to be attributed to various types of exogenous contamination, specifically, *APP* recombinant vectors, PCR products, and genome-wide mRNA contamination. Our replication experiment also showed the possibility of PCR amplification artifacts creating spurious products that mimic *APP* gene recombination with various internal exon junctions. Thus, to support the claimed phenomenon of *APP* gencDNA, it would be necessary for the authors to present unequivocal evidence that cannot be attributed to contamination, such as reads supporting novel *APP* insertion breakpoints; however, the authors have not presented such direct evidence. In conclusion, we found no evidence of *APP* retrotransposition in the genomic data presented in the Lee study and further show that our own single-neuron WGS analysis, which directly queried the *APP* locus at single-nucleotide resolution, reveals no evidence of *APP* retrotransposition or insertion.

Extended Data

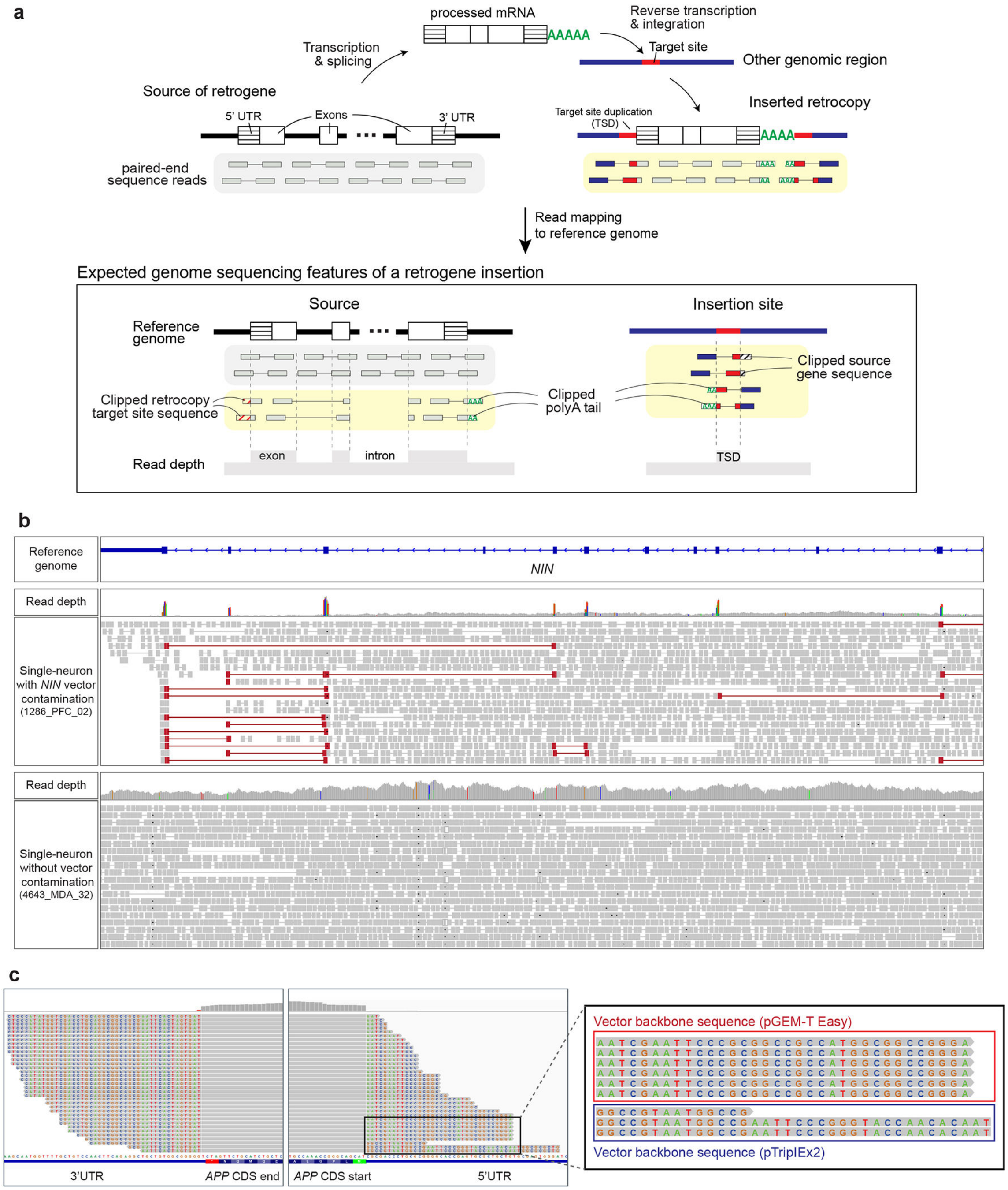

Extended Data Fig. 1. Pervasive recombinant vector contamination in next-generation sequencing.

a. Schematic of a retrogene insertion and the characteristics expected to be captured in sequencing data: increased exonic read-depth, discordant reads spanning exons, clipped reads at exon junctions, 3’ poly-A tail, target site duplication (TSD) at the new genomic insertion site, and clipped reads spanning the retrocopy and insertion sites. **b.** Recombinant vector contamination found in the Walsh laboratory data. Four single human neurons

(1286_PFC_02, 1762_PFC_04, 5379_PFC_01, 5416_PFC_06) in our previous publication showed contamination by a mouse *Nin* recombinant vector[15]. The homologous human gene region (*NIN*) is visualized by the IGV browser for a vector contaminated cell (upper panel) and an unaffected control cell (lower panel). Contamination characteristics were identified, including increased exonic read-depth and exon-spanning discordant reads (reads colored in red) with numerous mismatches to the human genome reference (colored vertical bars in the read depth track). **c.** Mouse single-neuron WGS data from the Chun laboratory[7] contaminated by the same *APP* recombinant vector detected in the Lee study[2] and an additional *APP* plasmid vector (magnified panel).

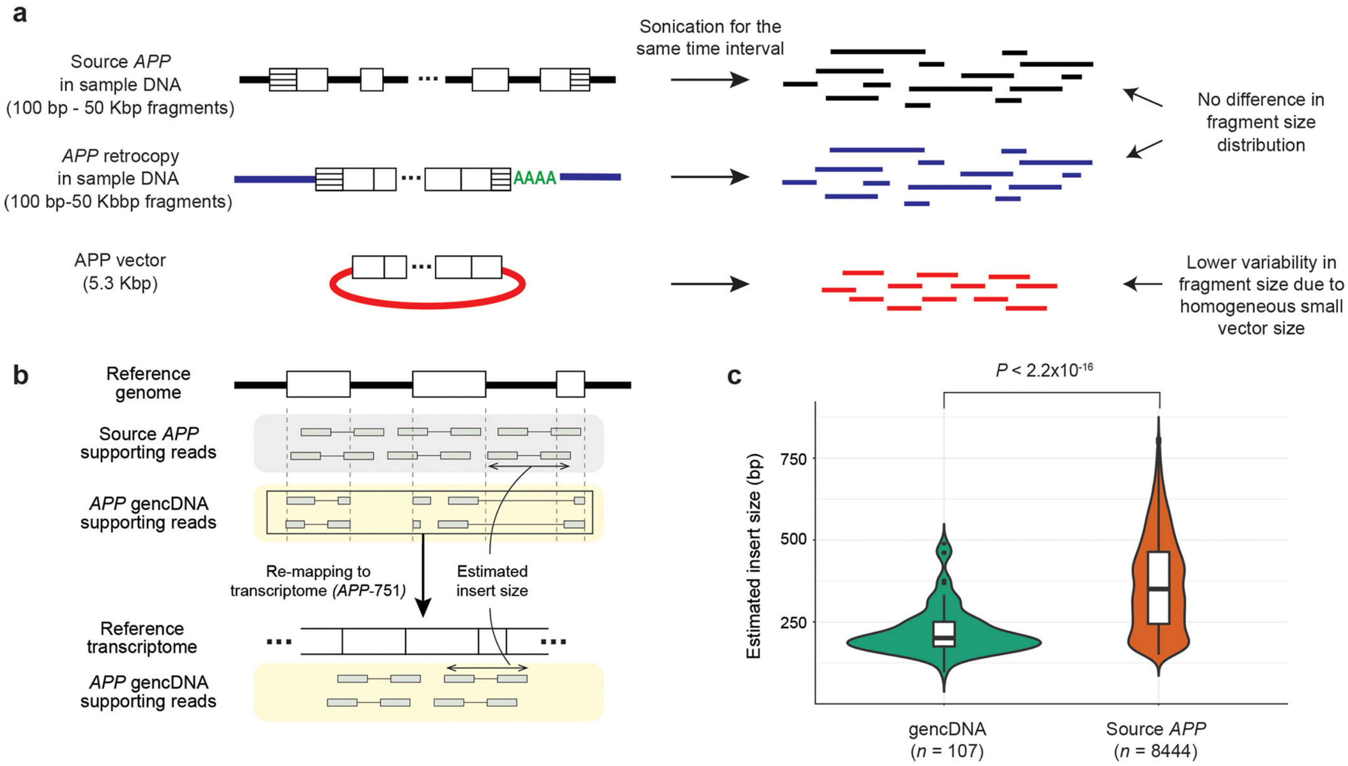

Extended Data Fig. 2. Evidence that recombinant vector contamination is the major source of *APP* gencDNA.

a. Schematic of the DNA fragment size distribution for each *APP* source (source *APP*, *APP* retrocopy, *APP* vector). Fragments from *APP* vectors are expected to be more homogeneous and smaller in size than those from other sources due to the fixed and relatively small vector size. **b.** DNA fragment (or insert) size estimation. Sequence reads mapped to *APP* exon junctions were divided into two groups: source *APP* (reads containing intron sequences) and *APP* gencDNA (reads clipped at the exon junction) supporting reads. gencDNA supporting reads were remapped to the *APP* reference transcript sequence (*APP*-751) to estimate insert sizes. **c.** Comparison of insert size distribution between source and gencDNA supporting reads. n, number of read pairs in each group.

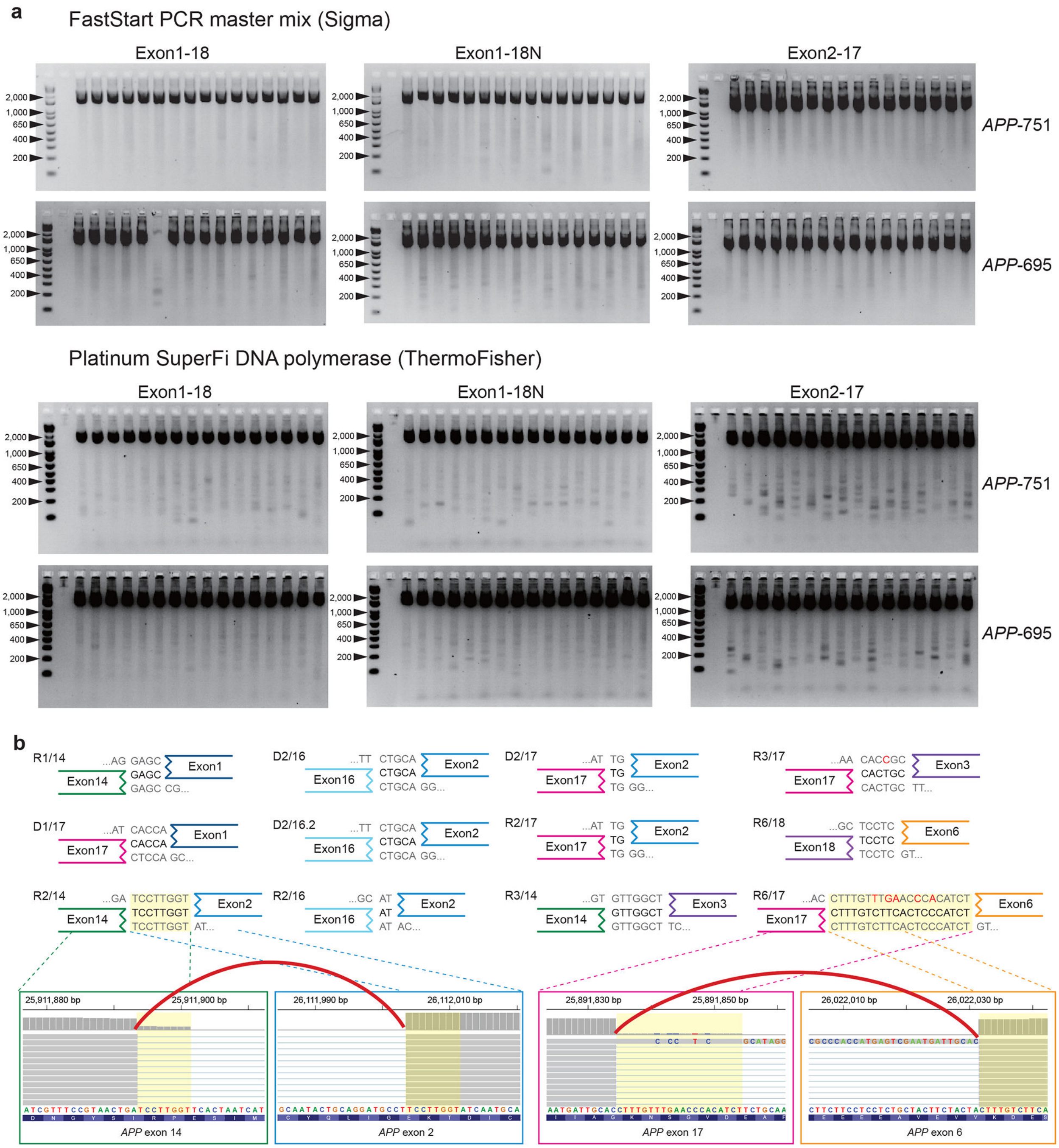

Extended Data Fig. 3. Novel *APP* variants with intra-exon junctions as PCR artifacts.

a. Electrophoresis of PCR products from the vector *APP* inserts (*APP*-751, *APP*-695) showing novel *APP* variants as artifacts. All combinations of two PCR enzymes (FastStart PCR master mix and Platinum SuperFi DNA polymerase; OneStep Ahead RT-PCR in Fig. 1c) with three primer sets generated novel bands smaller than the expected PCR product. **b.** PCR-induced IEJs with homologous sequences at each junction identified by Illumina sequencing. Twelve IEJs from our vector PCR sequencing showed the exact same sequence homologies and genomic coordinates as IEJs reported in the Lee study. For two IEJs, IGV browser images show pre- (left) and post-junction sites (right) connected by split reads spanning the IEJ (red arc). Because IGV displays forward strand sequences of the human reference genome, all IEJ sequences were also reverse complemented for consistent visualization.

Supplementary Material

Refer to Web version on PubMed Central for supplementary material.

Acknowledgements

This work was supported by NIA grant K01AG051791 and Suh Kyungbae Foundation (E.A.L.), NINDS grant R01NS032457-20S1 (C.A.W.), NIH grants T32HL007627 and K08AG065502 (M.B.M.), and NIH grant AG054748 (M.A.L). C.A.W. is an Investigator of the Howard Hughes Medical Institute.

Data availability

APP vector PCR sequences have been deposited in the NCBI Sequence Read Archive (PRJNA577966). Single-cell whole genome sequencing data of control individuals have been deposited in the NCBI Sequence Read Archive (PRJNA245456) and dbGAP (phs001485.v1.p1). Single-cell whole genome sequencing data of AD patients will be available upon request for genomic regions of *APP* and source pseudogene *SKA3* and *ZNF100*.

References

1. McConnell MJ et al. Intersection of diverse neuronal genomes and neuropsychiatric disease: The Brain Somatic Mosaicism Network. Science 356, doi:10.1126/science.aal1641 (2017).
2. Lee MH et al. Somatic APP gene recombination in Alzheimer's disease and normal neurons. Nature 563, 639–645, doi:10.1038/s41586-018-0718-6 (2018). [PubMed: 30464338]
3. Lee M-H et al. Reply: Evidence that APP gene copy number changes reflect recombinant vector contamination. bioRxiv, 730291, doi:10.1101/730291 (2019).
4. Park JS et al. Brain somatic mutations observed in Alzheimer's disease associated with aging and dysregulation of tau phosphorylation. Nat Commun 10, 3090, doi:10.1038/s41467-019-11000-7 (2019). [PubMed: 31300647]
5. Bushman DM et al. Genomic mosaicism with increased amyloid precursor protein (APP) gene copy number in single neurons from sporadic Alzheimer's disease brains. Elife 4, doi:10.7554/eLife.05116 (2015).
6. Kim J et al. Vecuum: identification and filtration of false somatic variants caused by recombinant vector contamination. Bioinformatics 32, 3072–3080, doi:10.1093/bioinformatics/btw383 (2016). [PubMed: 27334474]
7. Rohrback S et al. Submegabase copy number variations arise during cerebral cortical neurogenesis as revealed by single-cell whole-genome sequencing. Proc Natl Acad Sci U S A 115, 10804–10809, doi:10.1073/pnas.1812702115 (2018). [PubMed: 30262650]
8. Cooke SL et al. Processed pseudogenes acquired somatically during cancer development. Nat Commun 5, 3644, doi:10.1038/ncomms4644 (2014). [PubMed: 24714652]
9. Odelberg SJ, Weiss RB, Hata A & White R Template-switching during DNA synthesis by Thermus aquaticus DNA polymerase I. Nucleic Acids Res 23, 2049–2057, doi:10.1093/nar/23.11.2049 (1995). [PubMed: 7596836]
10. Evrony GD et al. Cell lineage analysis in human brain using endogenous retroelements. Neuron 85, 49–59, doi:10.1016/j.neuron.2014.12.028 (2015). [PubMed: 25569347]

11. Lodato MA et al. Aging and neurodegeneration are associated with increased mutations in single human neurons. Science 359, 555–559, doi:10.1126/science.aao4426 (2018). [PubMed: 29217584]

12. Erwin JA et al. L1-associated genomic regions are deleted in somatic cells of the healthy human brain. Nat Neurosci 19, 1583–1591, doi:10.1038/nn.4388 (2016). [PubMed: 27618310]

13. Evrony GD, Lee E, Park PJ & Walsh CA Resolving rates of mutation in the brain using single-neuron genomics. Elife 5, doi:10.7554/eLife.12966 (2016).

14. Zhao B et al. Somatic LINE-1 retrotransposition in cortical neurons and non-brain tissues of Rett patients and healthy individuals. PLoS Genet 15, e1008043, doi:10.1371/journal.pgen.1008043 (2019). [PubMed: 30973874]

15. Zhang X et al. Cell-Type-Specific Alternative Splicing Governs Cell Fate in the Developing Cerebral Cortex. Cell 166, 1147–1162 e1115, doi:10.1016/j.cell.2016.07.025 (2016). [PubMed: 27565344]

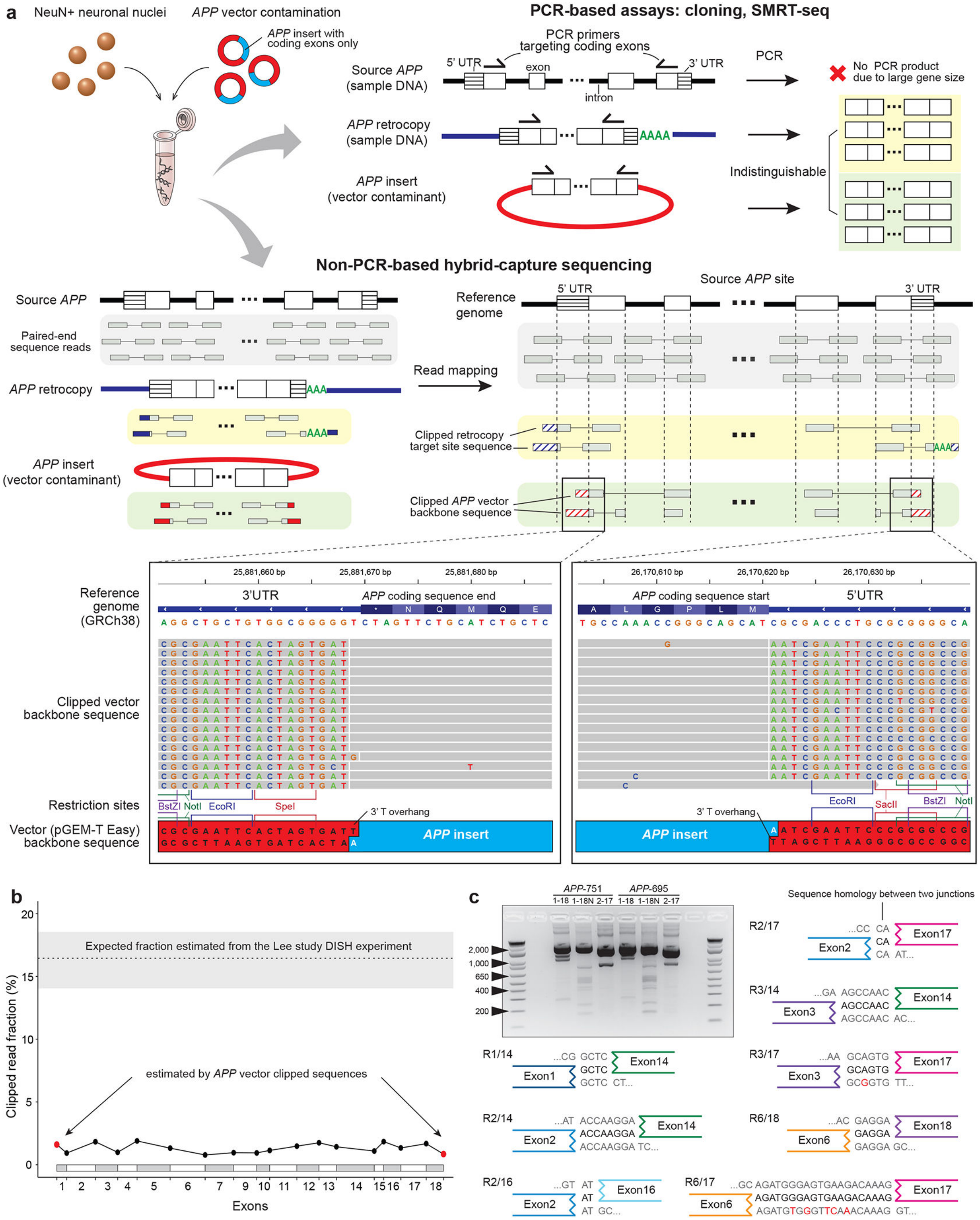
a
NeuN+ neuronal nuclei
APP vector contamination
APP insert with coding exons only
PCR-based assays: cloning, SMRT-seq
PCR primers targeting coding exons
Source APP (sample DNA)
5' UTR
exon
intron
3' UTR
PCR
No PCR product due to large gene size
APP retrocopy (sample DNA)
AAAA
APP insert (vector contaminant)
Indistinguishable
Non-PCR-based hybrid-capture sequencing
Source APP
Paired-end sequence reads
APP retrocopy
AAA
APP insert (vector contaminant)
Reference genome
Source APP site
5' UTR
3' UTR
Read mapping
Clipped retrocopy target site sequence
Clipped APP vector backbone sequence
Reference genome (GRCh38)
25,881,660 bp
25,881,670 bp
25,881,680 bp
3'UTR
APP coding sequence end
N Q M Q E
A G G C T G C T G T G G C G G G G G T C T A G T T C T G C A T C T G C T C
Clipped vector backbone sequence
C G C G A A T T C A C T A G T G A T
Restriction sites
BstZI NotI EcoRI SpeI
3' T overhang
Vector (pGEM-T Easy) backbone sequence
C G C G A A T T C A C T A G T G A T T
G C G C T T A A G T G A T C A C T A A
APP insert
26,170,610 bp
26,170,620 bp
26,170,630 bp
APP coding sequence start
5'UTR
A L G P L M
T G C C A A A C C G G G C A G C A T C G C G A C C C T G C G C G G G G C A
A A T C G A A T T C C C G C G G C C G
EcoRI SacII BstZI NotI
3' T overhang
APP insert
A A T C G A A T T C C C G C G G C C G
T T A G C T T A A G G G C G C C G G C
b
Expected fraction estimated from the Lee study DISH experiment
estimated by APP vector clipped sequences
Clipped read fraction (%)
0
5
10
15
20
1 2 3 4 5 6 7 8 9 10 11 12 13 14 15 16 17 18
Exons
c
APP-751
APP-695
1-18 1-18N 2-17 1-18 1-18N 2-17
2,000
1,000
650
400
200
Sequence homology between two junctions
R2/17
...CC CA
CA
CA AT...
Exon2
Exon17
R3/14
...GA AGCCAAC
AGCCAAC
AGCCAAC AC...
Exon3
Exon14
R1/14
...CG GCTC
GCTC
GCTC CT...
Exon1
Exon14
R3/17
...AA GCAGTG
GCAGTG
GCGGTG TT...
Exon3
Exon17
R2/14
...AT ACCAAGGA
ACCAAGGA
ACCAAGGA TC...
Exon2
Exon14
R6/18
...AC GAGGA
GAGGA
GAGGA GC...
Exon6
Exon18
R2/16
...GT AT
AT
AT GC...
Exon2
Exon16
R6/17
...GC AGATGGGAGTGAAGACAAAG
AGATGGGAGTGAAGACAAAG
AGATGTGGGTTCAAACAAAG GT...
Exon6
Exon17

Figure 1. *APP* vector contamination in the Lee study.

a. *APP* vector contamination and its manifestation in genome sequences. PCR-based assays in the Lee study fail to distinguish between *APP* retrocopy and vector *APP* insert. Hybrid-capture sequences from the Lee study shows clipped reads with a vector backbone sequence (pGEM-T Easy), including restriction sites at the multiple cloning site and a 3’ T-overhang. **b.** Estimated fractions of cells with *APP* gencDNA at the exon junctions in the Lee hybrid-capture data. All exon junction fractions (black dots) are comparable to the fraction at the coding sequence ends with vector backbone sequences (red dots). The dotted line on the top represents the conservative estimate of expected fraction based on the Lee DISH experiment (see Supplementary Methods); shaded area, 95% confidence interval. **c.** Electrophoresis and sequencing of PCR products from the vector *APP* inserts (*APP*-751/695) showing novel *APP* variants as artifacts. Eight out of 12 IEJs found both in our *APP* vector PCR sequencing and the Lee study RT-PCR results are shown (see also Extended Data Fig. 3).

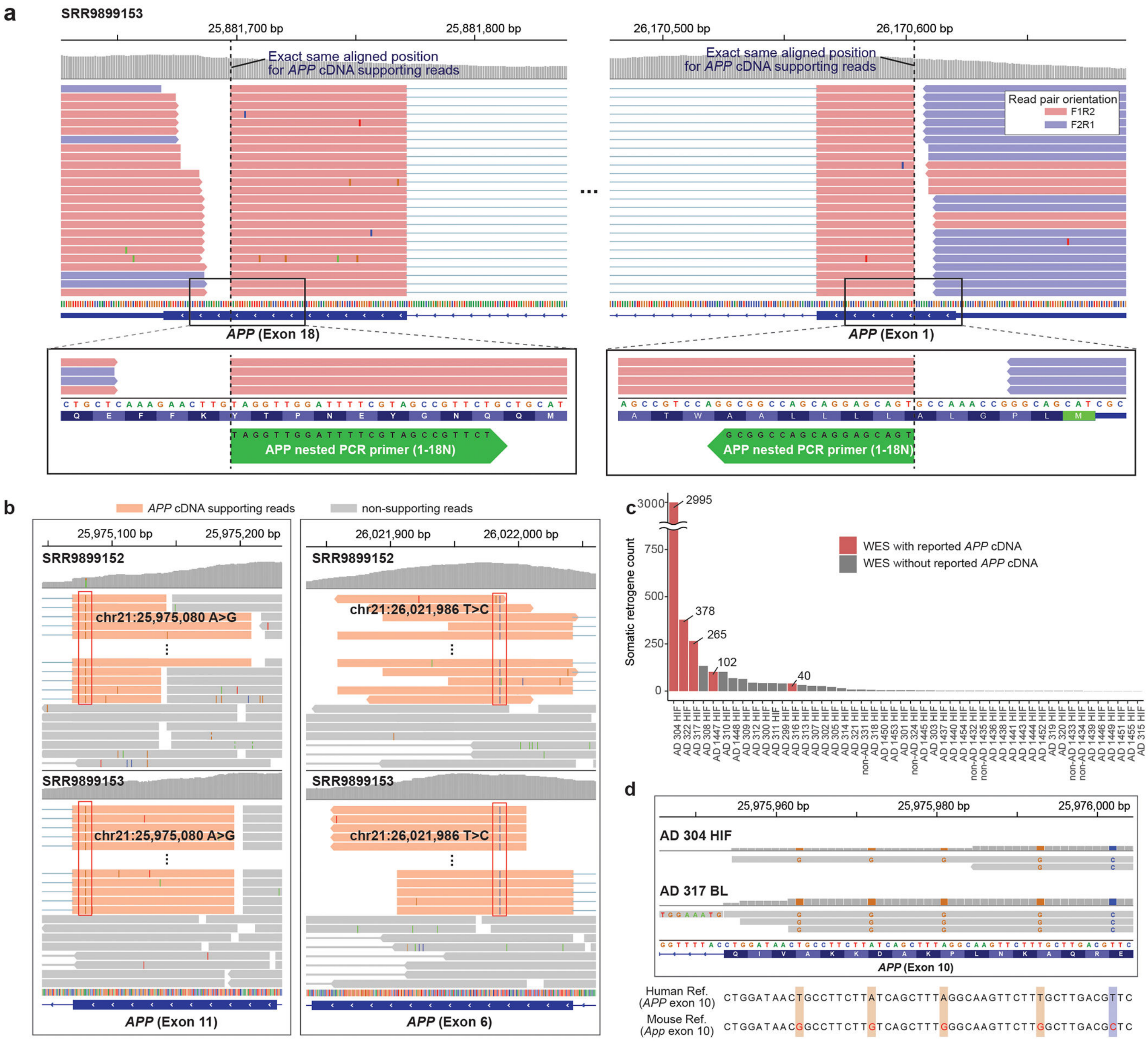

Figure 2. *APP* cDNA-supporting reads originate from exogenous PCR products and genome-wide human and mouse mRNA contamination.

a. *APP* nested PCR products found in the recent Lee WES data. Reads supporting *APP* cDNA are aligned to the target sites (dotted lines) of the nested PCR primers (green arrows at the bottom) used in the original Lee study. All these cDNA-supporting reads contain an IEJ between exon 2 and 17 (full structure not shown). **b.** The same unannotated variants found at two different positions (red boxes) only in cDNA supporting reads (orange) in both WES datasets by Lee et al. (SRR989152 and SRR989153). **c.** Total gene counts with potential somatic retrogene insertions in the Park et al. data. WES data with reported *APP* cDNA are marked in red. **d.** *APP* cDNA-supporting reads originating from mouse mRNA in the Park data. Mouse-specific single-nucleotide polymorphisms (colored bases) are observed in a portion of cDNA-supporting reads, including those with clipped sequences for exon-

exon junctions, suggesting the reads originated from mouse mRNA rather than genomic DNA (see also Supplementary Fig. 1).

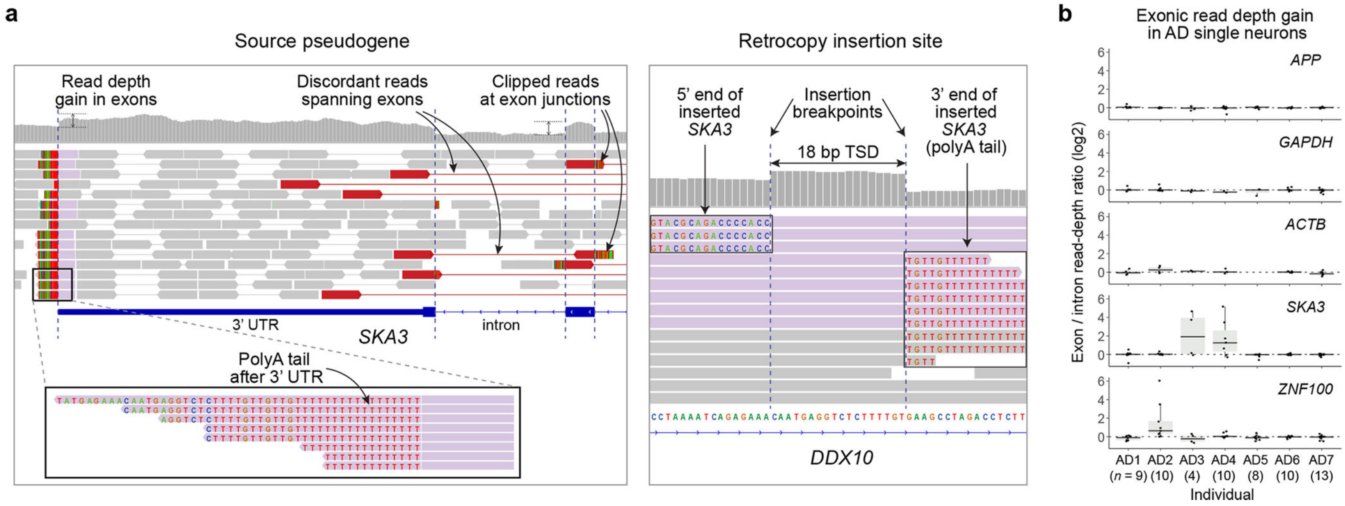

Figure 3. Absence of somatic *APP* retrogene insertions in our single-cell WGS data.

a. A germline pseudogene insertion (*SKA3*) in our scWGS data showing all distinctive characteristics of true retrogene insertion. **b.** No read-depth gain in *APP* exons in our AD single neurons. Each dot represents the median of exon/intron read-depth ratios across all exons of the gene in each scWGS dataset from AD patients. AD patients who have polymorphic germline retrogene insertions of *SKA3* (AD3 and AD4) and a germline insertion of *ZNF100* (AD2) show clear read-depth gain; no such gain for two housekeeping genes (*GAPDH*, *ACTB*). Single cells that had poor genomic coverage for a given gene due to locus dropout are excluded. n, number of single cells in each individual; center line, median; box limits, first and third quartiles.